Journal of Human Evolution 97 (2016) 17–26

Contents lists available at ScienceDirect

Journal of Human Evolution

journal homepage: www.elsevier.com/locate/jhevol

The evolutionary relationships and age of *Homo naledi*: An assessment using dated Bayesian phylogenetic methods

Mana Dembo [a, b, c, *], Davorka Radovčić [c, d], Heather M. Garvin [c, e, f], Myra F. Laird [c, g, h], Lauren Schroeder [c, i, j], Jill E. Scott [c, k, l], Juliet Brophy [c, m], Rebecca R. Ackermann [i, n], Chares M. Musiba [c, o], Darryl J. de Ruiter [c, p], Arne Ø. Mooers [a, q, **], Mark Collard [a, b, c, r, ***]

[a] *Human Evolutionary Studies Program, Simon Fraser University, 8888 University Drive, Burnaby, BC V5A 1S6, Canada*
[b] *Department of Archaeology, Simon Fraser University, 8888 University Drive, Burnaby, BC V5A 1S6, Canada*
[c] *Evolutionary Studies Institute and Centre for Excellence in PaleoSciences, University of the Witwatersrand, Private Bag 3, Wits 2050, South Africa*
[d] *Department of Geology and Paleontology, Croatian Natural History Museum, Demetrova 1, 10000 Zagreb, Croatia*
[e] *Department of Applied Forensic Sciences, Mercyhurst University, Erie, PA 16546, USA*
[f] *Department of Anthropology/Archaeology, Mercyhurst University, Erie, PA 16546, USA*
[g] *Center for the Study of Human Origins, Department of Anthropology, New York University, New York, NY 10003, USA*
[h] *New York Consortium in Evolutionary Primatology, New York, NY 10024, USA*
[i] *Department of Archaeology, University of Cape Town, Rondebosch 7701, South Africa*
[j] *Department of Anthropology, University at Buffalo SUNY, Buffalo, NY 14261, USA*
[k] *Department of Anthropology, The University of Iowa, Iowa City, IA 52242, USA*
[l] *Department of Sociology and Anthropology, Metropolitan State University of Denver, CO 80217-3362, USA*
[m] *Department of Geography and Anthropology, Louisiana State University, Baton Rouge, LA 70803, USA*
[n] *Human Evolution Research Institute, University of Cape Town, Rondebosch 7701, South Africa*
[o] *Department of Anthropology, University of Colorado, Denver, CO 80217, USA*
[p] *Department of Anthropology, Texas A&M University, College Station, TX 77843, USA*
[q] *Department of Biological Sciences, Simon Fraser University, 8888 University Drive, Burnaby, BC V5A 1S6, Canada*
[r] *Department of Archaeology, University of Aberdeen, St Mary's Building, Elphinstone Road, Aberdeen, AB24 3UF, UK*

ARTICLE INFO

Article history:
Received 21 August 2015
Accepted 29 April 2016

Keywords:
Dinaledi hominins
Bayesian phylogenetic analysis
Morphological clock
Genus *Homo*

ABSTRACT

Homo naledi is a recently discovered species of fossil hominin from South Africa. A considerable amount is already known about *H. naledi* but some important questions remain unanswered. Here we report a study that addressed two of them: "Where does *H. naledi* fit in the hominin evolutionary tree?" and "How old is it?" We used a large supermatrix of craniodental characters for both early and late hominin species and Bayesian phylogenetic techniques to carry out three analyses. First, we performed a dated Bayesian analysis to generate estimates of the evolutionary relationships of fossil hominins including *H. naledi*. Then we employed Bayes factor tests to compare the strength of support for hypotheses about the relationships of *H. naledi* suggested by the best-estimate trees. Lastly, we carried out a resampling analysis to assess the accuracy of the age estimate for *H. naledi* yielded by the dated Bayesian analysis. The analyses strongly supported the hypothesis that *H. naledi* forms a clade with the other *Homo* species and *Australopithecus sediba*. The analyses were more ambiguous regarding the position of *H. naledi* within the (*Homo*, *Au. sediba*) clade. A number of hypotheses were rejected, but several others were not. Based on the available craniodental data, *Homo antecessor*, Asian *Homo erectus*, *Homo habilis*, *Homo floresiensis*, *Homo sapiens*, and *Au. sediba* could all be the sister taxon of *H. naledi*. According to the dated Bayesian analysis, the most likely age for *H. naledi* is 912 ka. This age estimate was supported by the resampling analysis. Our findings have a number of implications. Most notably, they support the assignment of the new specimens to *Homo*, cast doubt on the claim that *H. naledi* is simply a variant of *H. erectus*, and suggest *H. naledi* is younger than has been previously proposed.

* Corresponding author
** Corresponding author
*** Corresponding author
E-mail addresses: mana.dembo@sfu.ca (M. Dembo), amooers@sfu.ca (A.Ø. Mooers), mcollard@sfu.ca (M. Collard).

http://dx.doi.org/10.1016/j.jhevol.2016.04.008
0047-2484/

1. Introduction

In late 2013 the fossilized remains of several hominin individuals were recovered from the Dinaledi chamber of the Rising Star cave system in the Cradle of Humankind World Heritage Site near Johannesburg, South Africa (Berger et al., 2015). Analyses of the craniodental and postcranial morphology of these individuals suggest that they share similarities with several species of *Homo*, including *Homo habilis*, *Homo rudolfensis, Homo erectus*, and *Homo heidelbergensis*, but are distinct enough to be assigned to a new species, which Berger et al. (2015) have named *Homo naledi*. So far it has not proved possible to obtain a radiometric or biostratigraphic date for *H. naledi* (Berger et al., 2015).

The discovery of a new hominin species raises a number of questions. One of the most important of these is "Where does the new species fit in the hominin evolutionary tree?" The answer to this question has the potential not only to shed new light on which species are our direct ancestors and which are our collateral relatives, but also illuminate the processes involved in hominin evolution. For example, phylogenetic analyses have shown that convergence has been an important factor in the evolution of the hominin skull (see e.g., Skelton and McHenry, 1992). In addition, the placement of a new species in the hominin evolutionary tree has taxonomic implications because most genus concepts hold that genera should be monophyletic (Collard and Wood, 2015).

Here, we report the first analysis of the phylogenetic relationships of *H. naledi*. Normally, palaeoanthropologists rely on maximum parsimony analysis to reconstruct hominin phylogenetic relationships (see e.g., Skelton and McHenry, 1992; Strait et al., 1997; Smith and Grine, 2008). However, while maximum parsimony analysis is useful for generating trees, it is not well suited to formally evaluating the relative support for different hypotheses of phylogenetic relationships, especially when fossil taxa are involved. With this in mind, we employed a relatively new, Bayesian inference-based method of phylogenetic analysis that allows phylogenetic hypotheses to be compared in a straightforward manner and with statistical rigor (Nylander et al., 2004; Pyron, 2011; Bergsten et al., 2013; Lee et al., 2014; Dembo et al., 2015). The Bayesian method of phylogenetic analysis (Rannala and Yang, 1996; Yang and Rannala, 1997) has been increasingly widely used over the last two decades to infer the relationships of extant organisms (see review by Huelsenbeck et al., 2008). Recently, its use has been extended to the study of the phylogenetic relationships of extinct taxa (Lee et al., 2014), including fossil hominins (Dembo et al., 2015).

The Bayesian method of phylogenetic analysis differs from maximum parsimony analysis in several respects. One difference concerns the treatment of character state changes. Maximum parsimony assumes that each character evolves via its own evolutionary process and therefore has its own rate of change along every branch of the tree (Steel and Penny, 2000). In contrast, common Bayesian methods require a single explicit model of character state change for all characters. The approaches also differ in relation to geological dates. In the maximum parsimony framework, geological dates can only be used a posteriori, by comparing the congruence of candidate trees and the stratigraphic record (Fisher, 2008). In contrast, geological dates can be used in the Bayesian framework to inform the expected amount of change leading to dated taxa at the inference stage (Ronquist et al., 2012a). A third crucial difference is the way in which trees are evaluated. Maximum parsimony relies on a single number—the minimum number of changes required to explain the observed differences. In the Bayesian approach, in contrast, trees are assessed and compared based on their posterior probability of being true given the data and the assumptions of the model of evolutionary change, with trees of higher probability being preferred. A recent simulation study showed that the Bayesian phylogenetic approach outperforms maximum parsimony when applied to discrete characters that are evolving at a high rate and when there are missing data (Wright and Hillis, 2014). Therefore, while further work is required to improve the model of the evolution of morphological data (see Section 4), Bayesian analysis can be expected to often produce more reliable hypotheses of relationships than maximum parsimony analysis.

Within the Bayesian framework, obtaining the posterior probability of a tree involves solving the following equation:

$$P(T,\theta|\,X) = \frac{P(X|T,\ \theta)P(T,\theta)}{P(X)} \tag{1}$$

where $P(T,\theta|X)$ represents the posterior probability of a particular tree (T) and the parameters (θ) given the data (X). The first term on the right, $P(X|T,\theta)$, is the likelihood function, which is the probability of observing the data given the candidate tree (T) and attendant parameters (θ). The second term, $P(T,\theta)$, is the prior probability of the tree and the parameters. $P(X)$ is the probability of the data across all possible trees and parameter values. For the second term in the numerator, we usually have few prior beliefs, and so most candidate trees and parameter values will be given equal prior probabilities. The term in the denominator is required because a Bayesian phylogenetic analysis returns a point probability for each tree and set of parameter values. The sum of these point probabilities across all possible trees and parameter values must equal 1.0. Unfortunately, we cannot calculate the overall probability of the data needed to calculate the posterior probabilities, because there is a near infinite number of possible combinations of trees and parameter values. Therefore, the posterior probabilities needed to evaluate trees (i.e., the entire right-hand side of equation (1)) are approximated using a sampling procedure known as the Markov chain Monte Carlo (MCMC) method (Yang and Rannala, 1997).

The MCMC method estimates the posterior probability of a tree as its frequency in a distribution of trees. Trees are evaluated and retained in this distribution in an iterative manner: a new tree or set of parameter values is proposed, and the resulting likelihood is multiplied by the prior probability of the tree and associated parameter values. The product is then compared to the corresponding value of the previously retained tree. If the fit to the data is better than that of the previous tree, the new tree and/or set of parameter values is retained. If it is worse, it is retained in proportion to how much worse it is (e.g., a topology that is 10X worse would have only a one in ten chance of being retained). Every time a new or unchanged tree is retained, the process is said to have produced a "generation" in a "chain," and the retained tree becomes the tree for comparison in a subsequent step. This is usually done over millions of steps, with good combinations of trees and parameter values being retained at high frequencies in the sample, suboptimal ones retained at lower frequency, and very poor ones ignored. Multiple chains can be constructed and compared in parallel, with some ("hot") chains being less likely to reject new candidate trees and parameters in the hope of sampling more broadly in search of optimal solutions (Beiko et al., 2006). Early on in a chain all trees may fit the data poorly, and so these early generations are usually discarded as "burn-in." Generally, while many millions of trees are evaluated and some large proportion retained, the distributions used in analyses are usually composed of trees from a smaller subsample, such as every 1000th tree in a chain. Known as the "posterior MCMC distribution," the retained subsample of trees and their attendant parameter values, prior

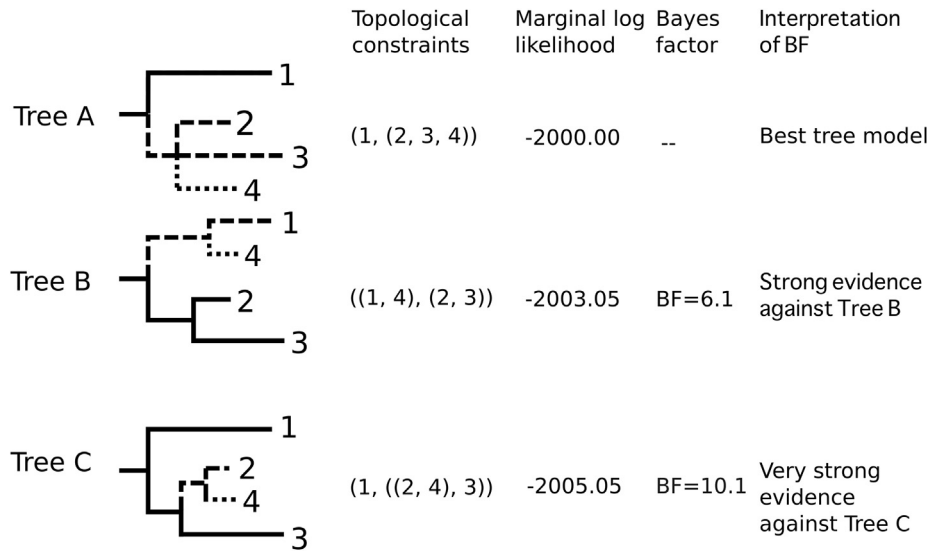

Figure 1. An illustration of how trees were constrained in the Bayes factor tests, and how we interpreted the Bayes factors yielded by the tests. Dotted edges are where the target species (4) can enter the corresponding model tree. For each hypothesis, we show one possible position after the data are analyzed. Bayes factor tests are carried out by comparing the marginal log likelihood of the best model tree to the other model trees. This figure is adapted from Dembo et al.'s (2015) Figure S1.

probabilities, and likelihoods allow the strength of support for individual clades to be evaluated and specific hypotheses to be compared (Bergsten et al., 2013).

In the study reported here, we employed two forms of Bayesian phylogenetic analysis. First, we conducted a dated Bayesian analysis. Developed over the last decade, this form of analysis is designed to work with samples that include fossil taxa (Pyron, 2011; Lee et al., 2014; Dembo et al., 2015). It uses geological dates associated with fossil specimens to constrain the branch lengths of non-contemporaneous[1] taxa (Lee et al., 2014) and therefore improve estimates of the rate of evolution. The trees sampled in a dated Bayesian analysis are summarized in a maximum clade credibility (MCC) tree, which shows the posterior probability for each clade. A clade's posterior probability is just the proportion of times the clade appears in trees in the MCMC sample. This means that the posterior probabilities of the MCC tree are coarse analogues of bootstrap values in the maximum parsimony framework.

Subsequently, we carried out a series of Bayes factor tests. A Bayes factor is a ratio of marginal likelihoods of two different hypotheses, and is interpreted as the relative ability of each hypothesis to predict the data (Kass and Raftery, 1995). A hypothesis that is more likely to lead to the observed dataset will produce a higher marginal likelihood than one that is less likely to have given rise to the observed dataset, and this will result in a high Bayes factor. In Bayes factor tests, competing hypotheses are represented as differing topological constraints on trees, and the aforementioned procedure for inferring trees is employed to produce the best fully defined hypotheses of relationship consistent with each constraint. The fits of these constrained trees to the data can then be compared. An advantage of this approach for palaeoanthropology is that ambiguity due to missing data simply leads to low Bayes factors, which indicates that the data cannot differentiate among trees (Dembo et al., 2015). In the present study, we used Bayes factor tests to compete hypotheses about the phylogenetic position of *H. naledi* suggested by the MCC tree. The hypotheses were converted into trees in the manner shown in Figure 1, and then the trees' marginal likelihoods were compared (Bergsten et al., 2013; Dembo et al., 2015).

The final part of our study focused on the age of the Dinaledi fossils. An unintended but useful byproduct of dated Bayesian analysis is a "morphological clock" estimate of the age of any undated terminal node. Such ages are produced by combining the rate of change for each character derived from the underlying model, the inferred tree, and the ages of geologically-dated terminal tips on the one hand with the character states exhibited by the undated tip on the other. While morphological data have been used in concert with molecular data to estimate the age of taxa without geological dates in a number of dated Bayesian analyses (e.g., Pyron, 2011; Ronquist et al., 2012a; Wood et al., 2013), we believe the exclusive use of morphological data to generate age estimates is novel, and remains untested (see discussion in Beck and Lee, 2014; Lee et al., 2014). With this in mind, we used a jackknife resampling procedure to assess the reliability of the morphological clock age for the Dinaledi fossils yielded by the dated Bayesian analysis.

2. Materials

2.1. Morphological data

Most of the data used in the study were taken from Dembo et al. (2015), who compiled a supermatrix from craniodental matrices used in 13 previous studies (Cameron and Groves, 2004; Cameron et al., 2004; Kimbel et al., 2004; Strait and Grine, 2004; Chang, 2005; Martinón-Torres et al., 2007; Gilbert, 2008; Argue et al., 2009; Mounier et al., 2009; Zeitoun, 2009; Berger et al., 2010; Irish et al., 2013; Lordkipanidze et al., 2013). When character state codes for a given character differed among studies, Dembo et al. (2015) resolved the disagreement by favouring codes from studies that used larger samples of fossils, that recognized more polymorphic states, and that employed simpler character scoring systems. When a conflict could not be resolved via these criteria, the taxon was coded as polymorphic for that character. For studies that reported character states for individual fossil specimens, Dembo et al. (2015) used a 66% majority-rule to code characters. If less than 66% of the specimens exhibited a given character state, the species was coded as polymorphic. This approach to merging matrices is conservative because it favours ambiguity whenever

[1] The term "non-contemporaneous" is used in the phylogenetics literature to refer to branches of the phylogeny that do not extend to the present (see, e.g., Wood et al., 2013).

there is disagreement among studies. In total, Dembo et al. (2015) assembled scores for 380 characters for 20 hominin taxa plus two extant hominoids, the gorilla (*Gorilla gorilla*), and the common chimpanzee (*Pan troglodytes*).

We made a number of alterations to the Dembo et al. (2015) supermatrix for the purposes of the present study. First, we merged two zygoma-related characters that we deemed too similar to be treated as independent characters. Second, we amended some of the codes for two characters related to the articular eminence. Third, we added codes for 12 additional characters for as many taxa as possible (characters 12, 46, 69, 105, 134, 258, 261, 272, 276–279 and 334 in Supplementary Online Material [SOM] Table S1). Seven of these characters relate to the cranium, five to the dentition, and one to the mandible. The additional characters were scored on original specimens and casts. Fourth, we added *H. naledi* to the matrix. We were able to score *H. naledi* for 123 of the characters, 73 cranial characters, 31 dental characters, and 19 mandibular characters. All 123 characters were scored on original specimens during a workshop held at the University of the Witwatersrand in May 2014. Where necessary, we adopted the 66% majority-rule to code *H. naledi*. Last, we used original specimens and casts to score several taxa for characters that were missing codes in the Dembo et al.'s (2015) supermatrix, paying particular attention to the 123 characters preserved in *H. naledi*. In total, the character state data matrix used in the present study contains scores for 391 craniodental characters for 22 hominin taxa and two extant hominoids (details of the fossil hypodigms are given in the SOM). This means that, to our knowledge, the dataset is the most comprehensive qualitative character state data matrix ever assembled for the tribe Hominini. The matrix and accompanying tables are provided in the SOM. They have also been deposited in the Dryad database (http://dx.doi.org/10.5061/dryad.d7r4g).

2.2. Geological dates

We used the oldest dates associated with the specimens that provided the morphological data to constrain the branch lengths for the non-*H. naledi* hominin taxa. Consequently, the dates used in this study (Table S2) do not necessarily correspond to the first appearance dates (FADs) of the taxa in the fossil record. In theory, dating the taxa on the basis of the oldest date associated with the specimens that provide the morphological data should link the scored character states with elapsed time more accurately than dating the taxa on the basis of the oldest known specimen in each hypodigm. This should, in turn, improve the estimates of the rate of evolutionary change for the characters (Ronquist et al., 2012a).

As we explained earlier, *H. naledi* has not been geologically dated (Berger et al., 2015). Consequently, we had to assign a date to it in a different manner. The analysis we carried out to do this is described below.

3. Analyses and results

3.1. Model parameter selection

Bayesian phylogenetic analyses are model based, so several decisions needed to be made before reconstructing the phylogeny of the hominins and evaluating the competing phylogenetic hypotheses concerning *H. naledi*. Specifically, we had to choose a model of character state evolution, and we had to select an appropriate clock model to infer the rate of change on the tree. Also, because *H. naledi* is currently undated, we had to decide how best to constrain it temporally.

We used a two-step procedure to choose the model of character state evolution, select a clock model, and temporally constrain *H. naledi*. First, we estimated the model likelihoods for the available options using MCMC simulation. We then compared the options using Bayes factors. A Bayes factor is calculated as twice the difference in natural logarithms of marginal likelihoods, and is interpreted on the same scale as the log-likelihood ratio test (Kass and Raftery, 1995). It is generally accepted that a Bayes factor greater than six suggests strong evidence in favour of one model over another; a Bayes factor greater than six indicates that the preferred model fits the data more than 400 times better than the alternative model (Kass and Raftery, 1995), and so is comparable to rejecting the alternative model at a p-value of less than 0.02. These analyses were conducted in MrBayes 3.2.4 (Ronquist et al., 2012b).

3.1.1. Process model Currently, only one widely-used model of character state change is available for discrete morphological data—Lewis's (2001) Markov k (Mk) state model. In the Mk model, characters switch among discrete states such that the probability of observing different states in a character is a truncated exponential function of time between observations.

Several of the parameters of the Mk model can be varied, and we assessed these parameters using Bayes factors before proceeding to tree generation and hypothesis comparison. One such parameter concerns characters that are phylogenetically uninformative. Morphological character state data matrices frequently include just those characters that have the potential to be informative regarding phylogenetic relationships. Characters that do not vary among the taxa and autapomorphic characters are often omitted. This sampling bias can be corrected in MrBayes by calculating conditional likelihoods based only on the parsimony-informative characters or characters with variable character states (Lewis, 2001; Nylander et al., 2004). Bayes factors (BF) indicated that the model with parsimony-informative correction was strongly preferred over both the model in which no sampling bias correction was implemented (BF = 723.28) and the model that assumed all variable characters were included (BF = 495.56). Thus, we opted to utilize the parsimony-informative correction option.

Another decision that needs to be made when implementing the Mk model is whether or not to allow characters to evolve at different rates. Heterogeneity in among-character rate of evolution can be modelled such that the rate of change for a given character can be sampled from a statistical distribution. Bayes factors strongly favoured the implementation of a gamma model of rate heterogeneity (Yang, 1994) over a model with a single rate of change assigned to all of the characters (BF = 24.84). Consequently, we implemented the model with a gamma distribution of rate heterogeneity.

3.1.2. Clock model In a dated Bayesian analysis, dates associated with fossil specimens are used to calibrate the rate of evolutionary change. This produces branch lengths that are proportional to time (Heath et al., 2014). MrBayes offers several clock models that differ in the assumptions they make about the rate of evolutionary change. The strict clock model assumes a constant rate of change throughout the tree (Zuckerkandl and Pauling, 1962). In contrast, in the relaxed clock model, the rate of change evolves through time. In the autocorrelated relaxed clock model (Thorne and Kishino, 2002), the descendant nodes evolve at a rate that is sampled from a distribution centred on the inferred rate of the ancestral branch. In the uncorrelated relaxed clock model (Drummond et al., 2006), the rate for each branch is sampled from an exponential distribution. Bayes factors indicated that the uncorrelated relaxed clock model was strongly preferred over the strict clock model (BF = 79.56), and that the uncorrelated relaxed clock model was better than the autocorrelated relaxed clock model (BF = 42.54). Based on these results, we decided to use the uncorrelated relaxed clock model in the main analyses.

The use of a relaxed clock model requires an additional parameter to model how nodes appear throughout the tree. A uniform prior on node times assumes that a node has equal probability of appearing across the interval between the time of its parent node and its oldest daughter node. A birth-death prior assumes that lineages arise and go extinct according to a stochastic process with parameters for speciation and extinction. Based on Bayes factors, the use of birth-death prior on node times was preferred over a uniform prior on node times (BF = 17.58), and we therefore included the prior probability of birth-death trees in our evaluation of candidate trees (see discussion of Equation (1) above).

Because *H. naledi* does not currently have an independent geological date, we used Bayes factor tests to assess four different potential age priors for this taxon. In the first model, we assumed that *H. naledi* could be as old as the oldest hominin species, and so *H. naledi* was assigned a uniform prior from 7.24 Ma (millions of years ago) to the present. In the second model, *H. naledi* was allowed to be as old as the oldest *Australopithecus* specimen in the sample, and thus the *H. naledi* node was given a uniform prior from 4.17 Ma to the present. In the third model, we assumed that *H. naledi* could be as old as the oldest specimen of the genus *Homo* for which we had morphological data. The age of the *H. naledi* terminal node was therefore assigned a uniform prior from 2.33 Ma to the present. In the last model, we treated *H. naledi* as a modern taxon. This model assumed that the *H. naledi* tip could not be older than the present. The Bayes factor tests indicated that there were no significant differences in the marginal likelihood values among the four models (Table 1 and Figs. S1–S4). Given this, we opted to use the "7.24 Ma to present" prior because it was the least likely to bias the placement of *H. naledi*.

3.2. Dated Bayesian analysis

Based on results of the preliminary analyses, we inferred trees using characters modelled to evolve under the Markov k model with a gamma-distributed among-character rate variation, correcting for the sampling bias for parsimony-informative characters. Of the 391 characters, 288 were treated as unordered and 103 as ordered. The polymorphic characters were treated as uncertainty in the character coding in the dated Bayesian analysis. The uncorrelated clock-model was employed to calibrate the tree, and the birth-death model was used as the prior on node times. We used a normally distributed clock rate prior with a mean of 0.2 and a standard deviation of 0.02. The hominin taxa were treated as non-contemporaneous tips to calibrate the clock, and the oldest dates associated with the specimens in the hypodigms used in this study were assigned as fixed ages for those terminal tips, except for the terminal node of *H. naledi*, which as explained above was assigned a uniform age prior between 7.24 Ma and the present.

We ran the Bayesian analysis in MrBayes 3.2.4. To estimate the posterior probability distribution of the trees and the parameters, we completed four independent runs, each with 20 million MCMC generations for each analysis. Each run consisted of one cold and three heated chains that could contribute to the cold chain, and we sampled the cold chain every 1000 generations. Convergence in the runs was assessed using MrBayes's convergence diagnostics and Tracer v.1.6 (Rambaut et al., 2014). All the standard test criteria were met (Tables S3–S6), indicating that convergence was achieved. We discarded the first 25% of the sampled trees in each run as burn-in.

The MCC tree, which summarizes the 60,000 post-burnin trees sampled during the Bayesian analysis, is presented in Figure 2. Several of the widely accepted relationships among the fossil hominins feature in this summary tree. For example, *Australopithecus anamensis* is the most basal species of the genus *Australopithecus* followed by *Australopithecus afarensis*. Similarly, the three *Paranthropus* species form a clade to the exclusion of all other hominin species, and *H. heidelbergensis*, *Homo neanderthalensis,* and *Homo sapiens* form a clade to the exclusion of other *Homo* species. The posterior probabilities for most of the relationships are low, but they are comparable to those obtained in other Bayesian phylogenetic studies involving morphological characters and a large percentage of fossil taxa with missing data (e.g., Lee et al., 2014).

In the MCC tree, *H. naledi* is found in a clade with the other *Homo* species and *Australopithecus sediba*. Within this clade, there is a split between *Homo floresiensis* and all the other species. There is then a split between a clade formed by *H. habilis* and *Au. sediba*, and one formed by the remaining *Homo* species. Within the latter clade, *H. naledi* is positioned as a member of a clade that also includes *Homo antecessor, H. heidelbergensis, H. neanderthalensis,* and *H. sapiens.* Thus, the MCC tree topology suggests that *H. naledi* is most closely related to *H. antecessor*, *H. heidelbergensis*, *H. neanderthalensis*, and *H. sapiens*, and that the closest relatives of the (*H. antecessor*, *H. heidelbergensis*, *H. naledi*, *H. neanderthalensis*, *H. sapiens*) clade are *H. erectus*, then *H. rudolfensis*, and then (*Au. sediba* plus *H. habilis)*. The MCC tree topology also suggests that the closest relative of the (*H. antecessor*, *H. erectus*, *H. habilis*, *H. heidelbergensis*, *H. naledi, H. neanderthalensis*, *H. rudolfensis*, *H. sapiens*, *Au. sediba*) clade is *H. floresiensis*.

3.3. Comparison with maximum parsimony and undated Bayesian analyses

Given that the Bayesian Mk method outperforms maximum parsimony when applied to discrete characters that are evolving at a high rate and when there are missing data (Wright and Hillis, 2014), it seems likely that a Bayesian analysis will produce more accurate reconstructions of fossil hominin phylogenetic relationships than a maximum parsimony analysis. As a check, we carried out two additional analyses: an undated Bayesian analysis and a maximum parsimony analysis. These analyses are reported in detail in the SOM. Briefly, the topological differences among the summary

Table 1
Different age prior settings for *H. naledi* used in this study.[a]

Models	Age prior (Ma)	Marginal likelihood	Bayes factor	Tip date (ka)	95% HPD on tip date (Ma)
As old as the oldest hominin	Uniform (0, 7.24)	−2563.66	BF = 1.52 No evidence to reject model	912	0–2.39
As old as the oldest australopith	Uniform (0, 4.17)	−2563.54	BF = 1.28 No evidence to reject model	909	0–2.37
As old as the oldest *Homo*	Uniform (0, 2.33)	−2563.10	BF = 0.40 No evidence to reject model	801	0–1.94
As extant species	Fixed (0)	−2562.90	Best model	0	–

[a] The marginal likelihoods and Bayes factors of the different age prior models evaluate the fit between the model and the data. The terminal date for the *H. naledi* branch is presented as the tip date along with the 95% high posterior density (HPD) interval.

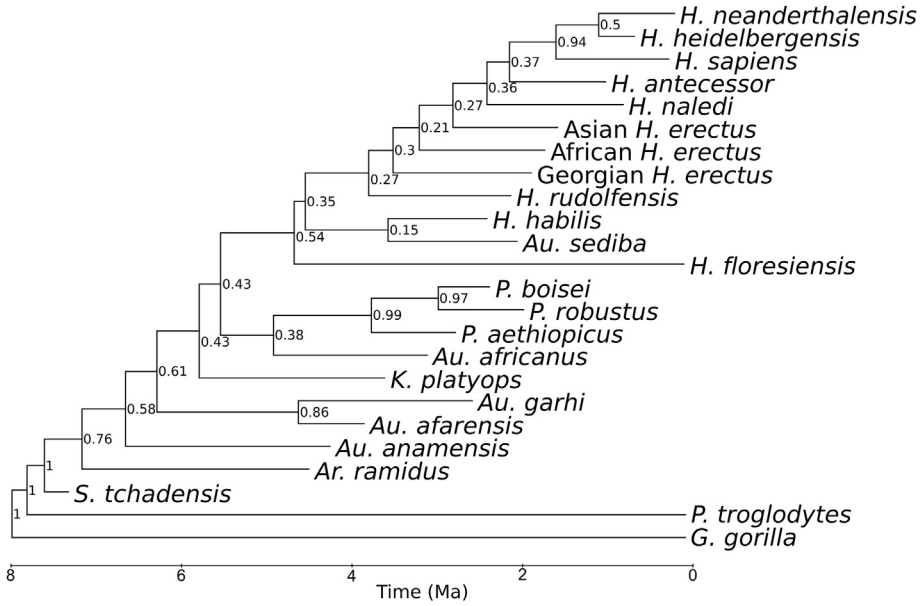

Figure 2. Summary of the best trees obtained in the dated Bayesian analysis. The posterior probability values for the clades are indicated.

trees yielded by the three analyses (Figs. 2, S5 and S7) are consistent with what we expect based on the differences among the methods (e.g., the use of a model of character evolution in the Bayesian analyses versus no model of character evolution in maximum parsimony analysis, and the use of FAD-constrained rates of evolutionary change in the dated Bayesian analysis versus unconstrained rates of evolutionary change in the undated Bayesian analysis). Such consistency lends further support to the Bayesian results. Less theoretically compelling but perhaps more intuitively satisfying, all three analyses place *H. naledi* in a clade with the widely recognized species of genus *Homo*.

3.4. Bayes factor tests

We carried out two Bayes factor tests. The goal of the first was to evaluate the strength of support for the hypothesis that *H. naledi* forms a clade with the other species of *Homo* and *Au. sediba*, as suggested by the MCC tree topology. Using the approach discussed earlier, we compared two hypothetical trees (Fig. S8). In one, the topology was constrained so that *H. naledi* was part of a clade that included the other *Homo* taxa (i.e., *H. antecessor*, African *H. erectus*, Asian *H. erectus*, Georgian *H. erectus*, *H. floresiensis*, *H. habilis*, *H. heidelbergensis*, *H. neanderthalensis*, *H. rudolfensis* and *H. sapiens*) and *Au. sediba.* In the other, the topology was constrained in such a way that *H. naledi* was excluded from a clade containing the other *Homo* taxa and *Au. sediba*.

In the second Bayes factor test, we assessed the strength of support for the potential sister group relationships of *H. naledi* within the (*Homo*, *Au. sediba*) clade (Fig. S9). To accomplish this we constructed hypothetical trees in which *H. naledi* was constrained to be the sister taxon of each of the other species in the (*Homo*, *Au. sediba*) clade, and then compared the strength of support for these trees in turn.

Some frequently used methods of estimating marginal likelihoods, such as the harmonic mean method (Newton and Raftery, 1994), are known to be biased and to overestimate marginal likelihoods (Xie et al., 2011; Baele et al., 2013). With this in mind, we took advantage of a new method (Stepping stone Importance Sampling) that allows for a broader sampling of the MCMC and provides a more accurate estimate of the marginal likelihoods (Fan et al., 2011; Xie et al., 2011). We used 50 steps, each consisting of 392,100 generations, with samples taken every 100 generations. The 3920 samples from the first of 50 steps were discarded as burn-in. The first 980 samples from all subsequent steps were also discarded for the same reason. For each stepping-stone sample, we conducted four independent runs. Each run involved one cold chain and three heated chains. The marginal likelihood was computed as the arithmetic mean of the four runs. The marginal likelihoods were then used to calculate the Bayes factor. Once again, the analyses were carried out in MrBayes 3.2.4.

The results of the first Bayes factor test were unambiguous (Table 2): they strongly support the indication from the MCC tree that *H. naledi* is nested within a clade consisting of the other *Homo* taxa and *Au. sediba* (BF = 10.22).

In the second set of Bayes factor tests, the tree in which *H. naledi* was constrained to be the sister of *Au. sediba* had the highest marginal likelihood. Compared to this tree, we were able to reject the trees in which *H. naledi* was constrained to be the sister taxon of African *H. erectus* (BF = 7.52), Georgian *H. erectus* (BF = 8.44), *H. heidelbergensis* (BF = 11.54), *H. neanderthalensis* (BF = 10.06), or *H. rudolfensis* (BF = 9.50). However, we could not reject the trees in which *H. naledi* was constrained to be the sister taxon of *H. antecessor*, Asian *H. erectus*, *H. habilis*, *H. floresiensis*, or *H. sapiens* (all BF < 6). Thus, the Bayes factor tests narrowed down the possibilities but did not identify the sister taxon of *H. naledi* within the (*Homo*, *Au. sediba*) clade. They indicated that *H. antecessor*, Asian *H. erectus*, *H. habilis*, *H. floresiensis*, *H. sapiens*, and *Au. sediba* could all be the sister taxon of *H. naledi*.

3.5. Estimating the age of H. naledi

Using the "7.24 Ma to present" prior, the dated Bayesian analysis placed the age of *H. naledi* at 912 ka (thousands of years ago), with a 95% high posterior density (HPD) interval between 0.000 and 2.388 Ma (Table 1).

To evaluate the accuracy of this estimate, we used a jackknife resampling procedure. This involved iteratively removing the geological dates associated with non-*H. naledi* hominin taxa to mimic the situation with regard to *H. naledi*, and then estimating the ages of non-*H. naledi* hominin taxa by dated Bayesian

Table 2
Results of the Bayes factor tests.[a]

	Marginal likelihood	Bayes factor	Interpretation
Is *H. naledi* nested in the clade of *Homo* + *Au. sediba*?			
Inside the clade	−2550.84	–	Best model
Outside the clade	−2555.95	10.22	Strong evidence to reject model
Does *H. naledi* form a sister taxon to other members of the genus *Homo* or *Au. sediba*?			
Sister to *H. antecessor*	−2556.04	0.24	Evidence not strong enough to reject model
Sister to African *H. erectus*	−2559.68	7.52	Strong evidence to reject model
Sister to Asian *H. erectus*	−2558.91	5.98	Evidence not strong enough to reject model
Sister to Georgian *H. erectus*	−2560.14	8.44	Strong evidence to reject model
Sister to *H. floresiensis*	−2557.68	3.52	Evidence not strong enough to reject model
Sister to *H. habilis*	−2558.90	5.96	Evidence not strong enough to reject model
Sister to *H. heidelbergensis*	−2561.69	11.54	Strong evidence to reject model
Sister to *H. neanderthalensis*	−2560.95	10.06	Strong evidence to reject model
Sister to *H. rudolfensis*	−2560.67	9.50	Strong evidence to reject model
Sister to *H. sapiens*	−2557.35	2.86	Evidence not strong enough to reject model
Sister to *Au. sediba*	−2555.92	–	Best model

[a] A Bayes factor greater than 6 indicates strong evidence against a tree model compared to the best model.

phylogenetic analysis. Subsequently, the estimated ages were statistically compared with the geological dates to assess the overall accuracy of the morphological clock.

Twenty hominin and two outgroup taxa were included in the jackknife analysis. The two hominin taxa that were excluded were *Sahelanthropus tchadensis* and *H. naledi.* Because we used the geological date associated with *S. tchadensis* as the upper limit of a uniform distribution for the root age of the hominins, there was reason to expect its morphological clock date would be biased towards younger ages. *Homo naledi* had to be excluded because it lacks a geological date.

Four independent, 20 million MCMC-generation runs were performed in each jackknife iteration. A “7.24 Ma to present” prior was used for the focal taxon in the MCMC analyses. Each MCMC run consisted of one cold and three heated chains that could contribute to the cold chain, and we sampled the cold chain every 1000 generations. Convergence in the runs was assessed using MrBayes's convergence diagnostics and Tracer v.1.6 (Rambaut et al., 2014). We discarded the first 25% of the sampled trees in each run as burn-in. Once the MCMC analyses were conducted, the tip date for the focal taxon was recorded. Subsequently, we used correlation analysis to compare all the morphological clock dates to the geological dates associated with the fossil taxa. The dated Bayesian analyses were carried out in MrBayes 3.2.4, while the inferred and geological ages were compared using Pearson correlation in the base R package (R Core Team, 2015).

The results of the morphological clock resampling analyses are presented in Figure 3 and Table 3. The dates estimated from the calibrated morphological clock are strongly correlated with the geological dates associated with the geological FADs for the hominin species ($r^2 = 0.56$). This supports the morphological clock age estimate of 912 ka for *H. naledi*.

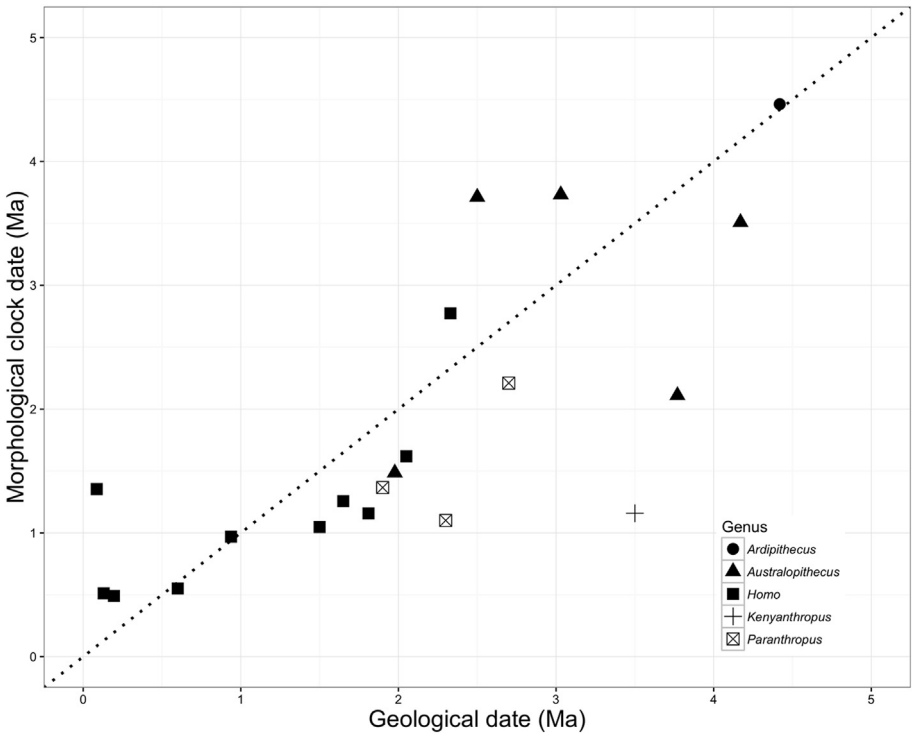

Figure 3. A plot of the geological dates associated with the fossil taxa compared with the dates estimated with the morphological clock. Points above the dotted line of equality represent species with dates that are overestimated by the morphological clock while points beneath the dotted line are species whose dates are underestimated by the morphological clock.

Table 3
Results of the resampling analysis to evaluate the accuracy of the morphological clock.[a]

Species	Geological date (Ma)	Morphological clock date (Ma)	Difference (millions of years)
Ardipithecus ramidus	4.419	4.463	0.044
Australopithecus anamensis	4.170	3.508	−0.662
Australopithecus afarensis	3.770	2.111	−1.659
Kenyanthropus platyops	3.500	1.159	−2.341
Australopithecus africanus	3.030	3.732	0.702
Paranthropus aethiopicus	2.700	2.210	−0.490
Australopithecus garhi	2.500	3.712	1.212
Homo habilis	2.330	2.773	0.443
Paranthropus boisei	2.300	1.101	−1.199
Homo rudolfensis	2.050	1.619	−0.431
Australopithecus sediba	1.977	1.486	−0.491
Paranthropus robustus	1.900	1.366	−0.534
Georgian *Homo erectus*	1.810	1.157	−0.653
African *Homo erectus*	1.650	1.257	−0.393
Asian *Homo erectus*	1.500	1.047	−0.453
Homo antecessor	0.938	0.969	0.031
Homo heidelbergensis	0.600	0.550	−0.050
Homo sapiens	0.195	0.491	0.296
Homo neanderthalensis	0.130	0.512	0.382
Homo floresiensis	0.019	1.354	1.335

[a] Dates were estimated from the calibrated morphological clock for each of the fossil hominin species. Positive values indicate a date overestimated by the morphological clock while the negative values indicate a date underestimated by the morphological clock.

It should be noted that the jackknife analysis was conducted prior to the publication of the new dates for *H. floresiensis* (Sutikna et al., 2016). As such, the geological date associated with *H. floresiensis* is younger 19 kya (Table 3). Using the new date for *H. floresiensis* in the correlation analysis did not have a significant impact on the r^2 value (it increased by just 0.004, from 0.564 to 0.568). This suggests that the new date is very unlikely to change the key findings of the present study.

4. Discussion

We investigated the phylogenetic relationships of the recently announced species *H. naledi* using a large supermatrix of craniodental characters and Bayesian phylogenetic methods. We began by inferring the phylogeny of all the fossil hominins. The 60,000 trees sampled during this analysis suggest that *H. naledi* is sister to a clade that includes *H. antecessor, H. heidelbergensis, H. neanderthalensis,* and *H. sapiens*, and that these species are nested within a clade formed by *Homo* species and *Au. sediba* (Fig. 2). Subsequently, we used Bayes factor tests to evaluate the hypothesis that *H. naledi* forms a clade with the other *Homo* taxa and *Au. sediba*, and to evaluate which taxon within this clade is most likely to be the sister of *H. naledi.* The Bayes factor tests supported the inclusion of *H. naledi* in a clade formed by the other *Homo* taxa and *Au. sediba*, but they did not support any particular sister taxon relationship between *H. naledi* and any of the other taxa in that clade. Rather, they indicated that *H. antecessor*, Asian *H. erectus*, *H. habilis*, *H. floresiensis*, *H. sapiens*, and *Au. sediba* could all be the sister taxon of *H. naledi*.

Berger et al. (2015) found that *H. naledi* shares craniodental features with several species of *Homo*, including *H. habilis*, *H. rudolfensis,* and *H. erectus*. Our results are consistent with this assessment to the extent that they support a close relationship between *H. naledi* and the other *Homo* taxa without linking *H. naledi* exclusively with any particular species within the *Homo* clade. However, our results depart from Berger et al.'s (2015) evaluation in some ways. The most obvious of these is that our Bayes factor analyses suggest that *H. naledi* is as closely related to *Au. sediba* as it is to some of the existing species of *Homo*. Our results are also inconsistent with a proposal that was put forward immediately following the publication of the initial description of the *H. naledi* fossils—namely that they do not represent a distinct species but instead belong to *H. erectus* (e.g., Zollikofer quoted in Randolph-Quinney, 2015). This hypothesis predicts that *H. naledi* should be either most closely related to African *H. erectus* or equally closely related to African *H. erectus*, Georgian *H. erectus*, and Asian *H. erectus*. However, the Bayes factor tests rejected the possibility that *H. naledi* is the sister taxon of African *H. erectus* and the possibility that it is the sister taxon of Georgian *H. erectus*. Thus, neither prediction of the "*H. erectus* hypothesis" is met. The most reasonable conclusion to draw from our phylogenetic results, we think, is that the position of *H. naledi* within the clade formed by *Homo* and *Au. sediba* is currently ambiguous. Improving the power of the supermatrix to discriminate among the various hypotheses should be a priority for future research.

The most likely age for *H. naledi* yielded by the dated Bayesian analysis (912 ka) was surprisingly well supported by the resampling procedure. This age estimate is considerably younger than has been proposed by Thackeray (2015) on the basis of the cranial characteristics of *H. naledi*. While our morphological clock date has to be treated with caution, there are interesting implications if *H. naledi* is indeed less than one million years old. Most obviously, it adds to the diversity of hominin species that persisted into more recent times. In addition, it expands the range of morphological variation observed among these later hominin species. Such a recent date for *H. naledi* suggests that small-brained *Homo* species lived contemporaneously with larger-brained *Homo* species in Africa, similar to the case in southeast Asia, with *H. floresiensis,* Asian *H. erectus*, and *H. sapiens* possibly all living contemporaneously (Brown et al., 2004).

The results of the present study have implications beyond the inclusion of *H. naledi* in a clade formed by *Homo* and *Au. sediba*, and the estimate of its age. Perhaps the most obvious of these concerns the genera to which *H. floresiensis* and *Au. sediba* are assigned. Given that the MCC tree recovered a clade formed by the various species of *Homo* and *Au. sediba*, with *H. floresiensis* as the most basal lineage, the species in the genus *Homo* may form a paraphyletic group. Since all of the genus concepts that are currently in use in palaeoanthropology agree that genera should be monophyletic (Collard and Wood, 2015), such a placement would suggest that either *Au. sediba* should be included in the genus *Homo* or *H. floresiensis* should be excluded from the genus. However, given

that we used only cranial characters in our analyses it would be sensible to revisit this issue after carrying out a phylogenetic analysis using a broader range of characters.

We conclude with a short list of suggestions for future research. One task concerns the low posterior probability values for parts of the MCC tree (Fig. 2). This may be due to the fact that the dataset has numerous empty cells and a large number of polymorphic characters. Alternatively, the low posterior values may be caused by the presence of "wildcard" taxa that move around in the trees. In addition, the dataset likely contains conflicting signals as a result of convergence, parallelism, and/or homoiology (Lieberman, 1999; Lockwood and Fleagle, 1999; Collard and Wood, 2001). Determining the influence of these contributors to low clade support will require further work. Reducing the number of empty cells in a data matrix that contains numerous fossil species is always going to be difficult. However, reducing the number of polymorphic characters should be easier, given that many arise because of disagreements among the datasets that were used to compile the supermatrix, and thus are likely due to differences of opinion among researchers. It should be possible to resolve many of these coding disagreements through quantification and statistical analysis. For those that cannot be resolved in this manner, the use of a panel of coders offers an interim way forward. If the MCC tree still has numerous low posterior probability values after the number of polymorphic characters has been reduced, it will be reasonable to conclude that conflicting signal among characters is the cause, with all that that implies.

A second avenue for future research is to add postcranial characters to the supermatrix. While our supermatrix is the largest qualitative dataset assembled to date, it contains only characters of the skull. The omission of postcranial data is problematic and these data should be added in future phylogenetic studies in order to assess total morphological pattern. The fossil material recovered from the Dinaledi chamber includes well-preserved postcranial remains with a unique combination of *Australopithecus*-like and *Homo*-like features (Berger et al., 2015; Harcourt-Smith et al., 2015; Kivell et al., 2015). As such, additional data on postcranial morphology may improve the power to discriminate among the hypotheses evaluated in the second part of this study.

Last, we need to develop better models of diversification and morphological character evolution. This process has already begun (e.g., Gavryushkina et al., 2014), but considerably more work is required. With regard to models of morphological character evolution, we know that various regions of the hominin cranium are integrated and so we expect covariation among cranial characters due to genetic, developmental, and functional constraints (Mitteroecker and Bookstein, 2008). But we do not have the relevant information to accommodate this in any phylogenetic inference framework at present. Fine-grained information on how shared developmental pathways influence covariation among craniodental characters would allow for a more complex model of character evolution in which the rates of evolution covary among characters and in different parts of the tree, analogous to the covarion models available for molecular data (Pagel and Meade, 2008). We suspect that models based on developmental data would significantly improve the support for hominin evolutionary relationships.

Acknowledgements

We wish to express our gratitude to the National Geographic Society and the National Research Foundation of South Africa for funding the discovery, recovery, and analysis of the *H. naledi* material. The study reported here was also made possible by grants from the Social Sciences and Humanities Research Council of Canada, the Canada Foundation for Innovation, the British Columbia Knowledge Development Fund, the Canada Research Chairs Program, Simon Fraser University, the DST/NRF Centre of Excellence in Palaeosciences (COE-Pal), as well as by a Discovery Grant from the Natural Sciences and Engineering Research Council of Canada, a Young Scientist Development Grant from the Paleontological Scientific Trust (PAST), a Baldwin Fellowship from the L.S.B. Leakey Foundation, and a Seed Grant and a Cornerstone Faculty Fellowship from the College of Liberal Arts, Texas A&M University. We would like to thank the South African Heritage Resource Agency for the permits necessary to work on the Rising Star site; the Jacobs family for granting access; Wilma Lawrence, Bonita De Klerk, Merrill Van der Walt, and Justin Mukanku for their assistance during all phases of the project; Lucas Delezene for valuable discussion on the dental characters of *H. naledi*. We would also like to thank Peter Schmid for the preparation of the Dinaledi fossil material; Yoel Rak for explaining in detail some of the characters used in previous studies; William Kimbel for drawing our attention to the possibility that there might be a problem with Dembo et al. (2015) codes for the two characters related to the articular eminence; Will Stein for helpful discussion about the Bayesian analyses; Mike Lee for his comments on this manuscript; John Hawks for his support in organizing the Rising Star workshop; and the associate editor and three anonymous reviewers for their valuable comments. We are grateful to S. Potze and the Ditsong Museum, B. Billings and the School of Anatomical Sciences at the University of the Witwatersrand, and B. Zipfel and the Evolutionary Studies Institute at the University of the Witwatersrand for providing access to the specimens in their care; the University of the Witwatersrand, the Evolutionary Studies Institute, and the South African National Centre of Excellence in PalaeoSciences for hosting a number of the authors while studying the material; and the Western Canada Research Grid for providing access to the high-performance computing facilities for the Bayesian analyses. Last but definitely not least, we thank the head of the Rising Star project, Lee Berger, for his leadership and support, and for encouraging us to pursue the study reported here.

Supplementary Online Material

Supplementary online material related to this article can be found at http://dx.doi.org/10.1016/j.jhevol.2016.04.008.

References

Argue, D., Morwood, M.J., Sutikna, T., Jatmiko, Saptomo, W., 2009. *Homo floresiensis*: a cladistic analysis. J. Hum. Evol. 57, 623–639.

Baele, G., Lemey, P., Vansteelandt, S., 2013. Make the most of your samples: Bayes factor estimators for high-dimensional models of sequence evolution. BMC Bioinform. 14, 85.

Beck, R.M.D., Lee, M.S.Y., 2014. Ancient dates or accelerated rates? Morphological clocks and the antiquity of placental mammals. Proc. R. Soc. B 281, 20141278.

Berger, L.R., de Ruiter, D.J., Churchill, S.E., Schmid, P., Carlson, K.J., Dirks, P.H.G.M., Kibii, J.M., 2010. *Australopithecus sediba*: a new species of *Homo*-like australopith from South Africa. Science 328, 195–204.

Berger, L.R., Hawkes, J., de Ruiter, D.J., Churchill, S.E., Schmid, P., Williams, S.A., DeSilva, J.M., Kivell, T.L., Skinner, M.M., Musiba, C.M., Cameron, N., Holliday, T.W., Harcourt-Smith, W.E.H., Ackermann, R.R., Bastir, M., Bogin, B., Bolter, D.R., Brophy, J.K., Cofran, Z.D., Congdon, K.A., Deane, A.S., Delezene, L.K., Dembo, M., Drapeau, M., Elliott, M.E., Feuerriegel, E.M., Garcia-Martinez, D., Garvin, H.M., Green, D.J., Gurtov, A.N., Irish, J.D., Kruger, A., Laird, M.F., Marchi, D., Meyer, M.R., Nalla, S., Negash, E.W., Orr, C.M., Radovčić, D., Schroeder, L., Scott, J.E., Throckmorton, Z., Tocheri, M.W., VanSickle, C., Walker, C.S., Wei, P., Zipfel, B., 2015. A new species of *Homo* from the Dinaledi Chamber, South Africa. eLife 4, 1–35.

Bergsten, J., Nilsson, A.N., Ronquist, F., 2013. Bayesian tests of topology hypotheses with an example from diving beetles. Syst. Biol. 62, 660–673.

Beiko, R.G., Keith, J.M., Harlow, T.J., Ragan, M.A., 2006. Searching for convergence in phylogenetic Markov chain Monte Carlo. Syst. Biol. 55, 553–565.

Brown, P., Sutikna, T., Morwood, M.J., Soejono, R.P., Jatmiko, Saptomo, E.W., Due, R.A., 2004. A new small-bodied hominin from the Late Pleistocene of Flores, Indonesia. Nature 431, 1055–1061.
Cameron, D.W., Groves, C.P., 2004. Bones, Stones and Molecules: Out of Africa and Human Origins. Elsevier, San Diego.
Cameron, D., Patnaik, R., Sahni, A., 2004. The phylogenetic significance of the Middle Pleistocene Narmada hominin cranium from central India. Int. J. Osteoarchaeol. 14, 419–447.
Chang, M.L., 2005. Neandertal origins, Middle Pleistocene systematics, and tests of current taxonomic and phylogenetic hypotheses. Ph.D. Dissertation, University of Pennsylvania.
Collard, M., Wood, B.A., 2001. Homoplasy and the early hominid masticatory system: inferences from analyses of extant hominoids and papionins. J. Hum. Evol. 41, 167–194.
Collard, M., Wood, B., 2015. Defining the genus *Homo*. In: Henke, W., Tattersall, I. (Eds.), Handbook of Paleoanthropology, 2nd ed. Springer Reference, New York, pp. 2107–2144.
Dembo, M., Matzke, N.J., Mooers, A.Ø., Collard, M., 2015. Bayesian analysis of a morphological supermatrix sheds light on controversial fossil hominin relationships. Proc. R. Soc. B 282, 20150943.
Drummond, A.J., Ho, S.Y.W., Phillips, M.J., Rambaut, A., 2006. Relaxed phylogenetics and dating with confidence. PLoS Biol. 4, e88.
Fan, Y., Wu, R., Chen, M.H., Kuo, L., Lewis, P.O., 2011. Choosing among partition models in Bayesian phylogenetics. Mol. Biol. Evol. 28, 523–532.
Fisher, D.C., 2008. Stratocladistics: integrating stratigraphic and morphologic data in phylogenetic inference. Annu. Rev. Ecol. Evol. Syst. 39, 365–385.
Gavryushkina, A., Welch, D., Stadler, T., Drummond, A.J., 2014. Bayesian inference of sampled ancestor trees for epidemiology and fossil calibration. PLoS Comput. Biol 10, e1003919.
Gilbert, W.H., 2008. *Homo erectus* cranial anatomy. In: Gilbert, W.H., Asfaw, B. (Eds.), *Homo erectus*: Pleistocene Evidence from the Middle Awash, Ethiopia. University of California Press, Berkeley, pp. 265–311.
Harcourt-Smith, W.E.H., Throckmorton, Z., Congdon, K.A., Zipfel, B., Deane, A.S., Drapeau, M., Churchill, S.E., Berger, L.R., DeSilva, J.M., 2015. The foot of *Homo naledi*. Nat. Commun. 6, 8432.
Heath, T.A., Huelsenbeck, J.P., Stadler, T., 2014. The fossilized birth–death process for coherent calibration of divergence-time estimates. Proc. Natl. Acad. Sci. 111, E2957–E2966.
Huelsenbeck, J.P., Ronquist, F., Nielsen, R., Bollback, J.P., 2008. Bayesian inference of phylogeny and its impact on evolutionary biology. Science 294, 2310–2314.
Irish, J.D., Guatelli-Steinberg, D., Legge, S.S., de Ruiter, D.J., Berger, L.R., 2013. Dental morphology and the phylogenetic "place" of *Australopithecus sediba*. Science 340, 1233062.
Kass, R.E., Raftery, A.E., 1995. Bayes factors. J. Am. Stat. Assoc. 90, 773–795.
Kimbel, W.H., Rak, Y., Johanson, D.C., 2004. The Skull of *Australopithecus afarensis*. Oxford University Press, New York.
Kivell, T.L., Deane, A.S., Tocheri, M.W., Orr, C.M., Schmid, P., Hawkes, J., Berger, L.R., Churchill, S.E., 2015. The hand of *Homo naledi*. Nat. Commun. 6, 8431.
Lee, M.S.Y., Cau, A., Naish, D., Dyke, G.J., 2014. Morphological clocks in paleontology, and a mid-Cretaceous origin of crown Aves. Syst. Biol. 63, 442–449.
Lewis, P.O., 2001. A likelihood approach to estimating phylogeny from discrete morphological character data. Syst. Biol. 50, 913–925.
Lieberman, D.E., 1999. Homology and hominid phylogeny: problems and potential solutions. Evol. Anthropol. 7, 142–151.
Lockwood, C.A., Fleagle, J.G., 1999. The recognition and evaluation of homoplasy in primate and human evolution. Yearb. Phys. Anthropol. 42, 189–232.
Lordkipanidze, D., Ponce de León, M.S., Margvelashvili, A., Rak, Y., Rightmire, G.P., Vekua, A., Zollikofer, C.P.E., 2013. A complete skull from Dmanisi, Georgia, and the evolutionary biology of early *Homo*. Science 342, 326–331.
Martinón-Torres, M., Bermúdez de Castro, J.M., Gomez-Robles, A., Arsuaga, J.L., Carbonell, E., Lordkipanidze, D., Manzi, G., Margvelashvili, A., 2007. Dental evidence on the hominin dispersals during the Pleistocene. Proc. Natl. Acad Sci. 104, 13279–13282.
Mitteroecker, P., Bookstein, F., 2008. The evolutionary role of modularity and integration in the hominoid cranium. Evolution 62, 943–958.
Mounier, A., Marchal, F., Condemi, S., 2009. Is *Homo heidelbergensis* a distinct species? New insight on the Mauer mandible. J. Hum. Evol. 56, 219–246.
Newton, M.A., Raftery, A.E., 1994. Approximante Bayesian Inference with the weighted likelihood bootstrap. J. R. Stat. Soc. B 56, 3–48.
Nylander, J., Ronquist, F., Huelsenbeck, J., Nieves-Aldrey, J., 2004. Bayesian phylogenetic analysis of combined data. Syst. Biol. 53, 47–67.
Pagel, M., Meade, A., 2008. Modelling heterotachy in phylogenetic inference by reversible-jump Markov chain Monte Carlo. Phil. Trans. R. Soc B 363, 3955–3964.
Pyron, R.A., 2011. Divergence time estimation using fossils as terminal taxa and the origins of Lissamphibia. Syst. Biol. 60, 466–481.
R Core Team, 2015. R: A language and environment for statistical computing. R Foundation for Statistical Computing, Vienna, Austria. URL. http://www.R-project.org/.
Rambaut, A., Suchard, M.A., Xie, D., Drummond, A.J., 2014. Tracer v1.6. Available from. http://beast.bio.ed.ac.uk/Tracer.
Randolph-Quinney, P.S., 2015. The mournful ape: conflating expression and meaning in the mortuary behaviour of *Homo naledi*. S. Afr. J. Sci. 111, 1–5.
Rannala, B., Yang, Z., 1996. Probability distribution of molecular evolutionary trees: a new method of phylogenetic inference. J. Mol. Evol. 43, 304–311.
Ronquist, F., Klopfstein, S., Vilhelmsen, L., Schulmeister, S., Murray, D.L., Rasnitsyn, A.P., 2012a. A total-evidence approach to dating with fossils, applied to the early radiation of the Hymenoptera. Syst. Biol. 61, 973–999.
Ronquist, F., Teslenko, M., van der Mark, P., Ayres, D.L., Darling, A., Höhna, S., Larget, B., Liu, L., Suchard, M.A., Huelsenbeck, J.P., 2012b. MrBayes 3.2: efficient Bayesian phylogenetic inference and model choice across a large model space. Syst. Biol. 61, 539–542.
Skelton, R.R., McHenry, H.M., 1992. Evolutionary relationships among early hominids. J. Hum. Evol. 23, 309–349.
Smith, H.F., Grine, F.E., 2008. Cladistic analysis of early *Homo* crania from Swartkrans and Sterkfontein, South Africa. J. Hum. Evol. 54, 684–704.
Steel, M., Penny, D., 2000. Parsimony, likelihood, and the role of models in molecular phylogenetics. Mol. Biol. Evol. 17, 839–850.
Strait, D.S., Grine, F.E., 2004. Inferring hominoid and early hominid phylogeny using craniodental characters: the role of fossil taxa. J. Hum. Evol. 47, 399–452.
Strait, D.S., Grine, F.E., Moniz, M.A., 1997. A reappraisal of early hominid phylogeny. J. Hum. Evol. 32, 17–82.
Sutikna, T., Tocheri, M.W., Morwood, M.J., Saptomo, E.W., Jatmiko, Awe, R.D., Wasisto, S., Westaway, K.E., Aubert, M., Li, B., Zhao, J., Storey, M., Alloway, B.V., Morley, M.W., Meijer, H.J.M., van den Bergh, G.D., Grün, R., Dosseto, A., Brumm, A., Jungers, W.L., Roberts, R.G., 2016. Revised stratigraphy and chronology for *Homo floresiensis* at Liang Bua in Indonesia. Nature 532, 366–369.
Thackeray, J.F., 2015. Estimating the age and affinities of *Homo naledi*. S. Afr. J. Sci. 111, 11–12.
Thorne, J.L., Kishino, H., 2002. Divergence time and evolutionary rate estimation with multilocus data. Syst. Biol. 51, 689–702.
Wood, H.M., Matzke, N.J., Gillespie, R.G., Griswold, C.E., 2013. Treating fossils as terminal taxa in divergence time estimation reveals ancient vicariance patterns in the palpimnoid spiders. Syst. Biol. 62, 264–284.
Wright, A.M., Hillis, D.M., 2014. Bayesian analysis using a simple likelihood model outperforms parsimony for estimation of phylogeny from discrete morphological data. PLoS One 9, e109210.
Xie, W., Lewis, P.O., Fan, Y., Kuo, L., Chen, M.H., 2011. Improving marginal likelihood estimation for Bayesian phylogenetic model selection. Syst. Biol. 60, 150–160.
Yang, Z., 1994. Maximum likelihood phylogenetic estimation from DNA sequences with variable rates over sites: approximate methods. J. Mol. Evol. 39, 306–314.
Yang, Z., Rannala, B., 1997. Bayesian phylogenetic inference using DNA sequences: a Markov chain Monte Carlo method. Mol. Biol. Evol. 14, 717–724.
Zeitoun, V., 2009. The Human Canopy: *Homo erectus*, *Homo soloensis*, *Homo pekinensis* and *Homo floresiensis*. J. and E. Hedges, Oxford.
Zuckerkandl, E., Pauling, L., 1962. Molecular disease, evolution, and genetic heterogeneity. In: Kasha, M., Pullman, B. (Eds.), Horizons in Biochemistry. Academic Press, New York, pp. 189–225.